Carbohydrate Polymers 111 (2014) 101–107

Contents lists available at ScienceDirect

Carbohydrate Polymers

journal homepage: www.elsevier.com/locate/carbpol

A robust pH-sensitive drug carrier: Aqueous micelles mineralized by calcium phosphate based on chitosan

Yan Lv, Hailong Huang, Bohan Yang, Huan Liu, Yapeng Li*, Jingyuan Wang

Alan G. MacDiarmid Institute of Jilin University, 2699 Qianjin Street, 130012 Changchun, China

ARTICLE INFO

Article history:
Received 27 September 2013
Received in revised form 21 April 2014
Accepted 21 April 2014
Available online 28 April 2014

Chemical compounds studied in this article:
Doxorubicin hydrochloride (PubChem CID: 443939)
Polyethylene glycol monomethyl ether (PubChem CID: 174)
Dodecylamine (PubChem CID: 443939)

Keywords:
Chitosan
Calcium phosphate
Drug release
pH-sensitive

ABSTRACT

This study developed an exciting alternative to the polymeric delivery system in cancer therapy. In this study, novel organic–inorganic hybrid polymeric micelles based on chitosan were synthesized and found to be robust nanocarriers for intracellular controlled release drug delivery. The polymeric micelles of carboxymethyl chitosan-grafted-p(ethylene glycol)-dodecylamine (CMC-g-PEG-DDA) were readily mineralized in the presence of calcium chloride ($CaCl_2$) and disodium hydrogen phosphate (Na_2HPO_4). Mineralization reduced polymeric micelles' size from 239 nm to 138 nm and formed a multi-core structure. The mineralized polymeric micelles (MPM) exhibited enhanced serum stability. The DOX release from the DOX-loaded mineralized polymeric micelles (MPM@DOX) at physiological pH was efficiently inhibited, At an endosomal pH (pH 5.0), DOX release was facilitated due to rapid dissolution of the calcium phosphate (CaP). These results indicate that mineralized polymeric micelles are potentially as robust carriers that can release DOX at specific sites under mild acidic conditions, such as in an extracellular matrix of tumor tissue and intracellular cell compartments.

1. Introduction

Self-assembled polymeric nanoparticles composed of amphiphilic polymers have been investigated for use in cancer therapy since they permit the encapsulation of a mass of hydrophobic therapeutic agents (Adams, Lavasanifar, & Kwon, 2003; Choi et al., 2010; Shi, Votruba, Farokhzad, & Langer, 2010). However, the stability of self-assembled nanoparticles has not been clearly proven (Bae & Yin, 2008). They have a limited ability to eradicate tumors because nanoparticles may release a considerable portion of the anticancer drugs before they are taken up by tumor cells (Yuk et al., 2012). To overcome these limitations, many studies have focused on the preparation of smart nanoparticles such as the environmentally responsive nanoparticles, nanoparticles bearing tumor-targeting moieties and organic-inorganic hybrid nanomaterials (Fan et al., 2010; Onaca, Enea, Hughes, & Meier, 2009; Perkin, Turner, Wooley, Mann, & Stephen, 2005).

The development of organic–inorganic hybrid nanomaterials is of great interest in the field of biotechnology. One of the organic-inorganic hybrid nanomaterials is making biocompatible inorganic components deposit on self-assembled polymer nanotemplates. They can used as functional nanocarriers for bioactive agents including drugs, genes and imaging agent (Li, Chen, & Liu, 2013; Qutachi, Shakesheff, & Buttery, 2013; Sugawara, Yamane, & Akiyoshi, 2006) Calcium phosphate(CaP)-based biomineralized nanoparticles are promising candidates for drug delivery systems due to their excellent biocompatibility (Epple et al., 2010).

CaP is superior to other inorganic species such as silica in terms of biocompatibility, since CaP is naturally found as the main mineral component in bone. In addition, CaP is absorbable in specific cellular environments (endosome/lysosome) as non-toxic ionic species (Han et al., 2013; Lee et al., 2010). Another interesting property is the aqueous solubility of CaP, which is largely dependent on pH. As pH decreases, solubility increases exponentially. CaP maintains its mineral structure at a physiological pH and dissolves in acidic pH environments like intracellular endosomes and lysosomes (pH 4.5) (Angelos, Yang, Patel, Stoddart, & Zink, 2008). This pH-dependent dissolution behavior can be incorporated into nanocarriers to produce useful intracellular drug delivery systems. Therefore, combining controlled mineralization technology with self-assembled polymer nanotemplates can facilitate the development of nanocarriers for drug delivery that are robust, pH-sensitive, biocompatible and biodegradable.

* Corresponding author. Tel.: +86 0431 85168238; fax: +86 0431 85168238.
E-mail address: liyapeng@jlu.edu.cn (Y. Li).

http://dx.doi.org/10.1016/j.carbpol.2014.04.082
0144-8617/

Chitosan is a linear, cationic polysaccharide which is a natural polymer. Due to its advantageous properties including biodegradability, biocompatibility, bioadhesivity and nontoxicity, chitosan has attracted much attention as a novel drug-carrier system for cancer therapy (Kurita, 2001; Wang et al., 2013). However, unmodified chitosan is only soluble at an acidic pH(<6),which limits its many applications (Yao, Zhang, Ping, & Yu, 2007). To overcome this limitation, we synthesized an amphiphilic polymer, carboxymethyl chitosan-grafted-p(ethyleneglycol)-dodecylamine (CMC-g-PEG-DDA), which has good solubility in aqueous and organic solution (DMSO). PEGylated polymers may improve the stability of drug delivery systems in the blood by preventing the absorption of protein and uptake by reticuloendothelial systems (RES) (Hiki & Kataoka, 2007; Hu et al., 2008). Dodecylamine (DDA) could encapsulate a large amount of hydrophobic therapeutic agents, which can control the size of nanoparticles. In this study, unmodified carboxylate groups in carboxymethyl chitosan were used to preorganize Ca^{2+} ions and initiate onset of calcium phosphate nucleation (Rim, Min, Lee, Jeong, & Lee, 2011; Schmidt & Ostafin, 2002).

This paper describes the spatially selective mineralization of polymeric micelles to produce highly biocompatible, robust hybrid nanocarriers that can controllably release anticancer drugs. The physicochemical properties of calcium phosphate mineralized nanoparticals were characterized with FT-IR, thermogravimetric analysis (TGA), transmission electron microscopy (TEM), dynamic light scattering (DLS), and energy-dispersive X-ray photoelectron spectroscopy (EDS). Doxorubicin (DOX), chosen as the model anticancer drug, was encapsulated in the (M)PM with the dialysis method, and the effect of the pH on DOX release from the mineralized polymeric micelles was evaluated.

2. Materials and methods

2.1. Materials

Chitosan (CS) was provided by Shanghai Kabo Biochemical (China), with a degree of deacetylation of 90% and viscosity-average molecular weight of 50,000 Da. Polyethylene glycol monomethyl ether (mPEG (2000)-OH) was obtained from Sigma. In addition, 1-ethyl-3-(3-dimethylaminopropyl) carbodiimide (EDC) and dodecylamine (DDA) were obtained from Aldrich. Carboxymethyl chitosan (CMC) was synthesized according to Shi, Shen, Zhang, Bi, and Dai (2012). (According to the ratio of the peak area at 3.99 ppm to that at 2.9 ppm in the ^{1}H NMR spectrum in Fig. S1, the substitution of carboxymethyl group was 71%.) Details are described in the supporting information (Fig. S1). The anti-cancer drug doxorubicin (DOX) hydrochloride was purchased from Pfizer, China. Calcium chloride ($CaCl_2$) and disodium hydrogen phosphate (Na_2HPO_4) were of the reagent grade. Dimethyl sulfoxide (DMSO) was purchased from Beijing Chemical works (China) with further purification prior to use.

2.2. Synthesis and characterization of carboxymethyl chitosan-grafted-p(ethyleneglycol)-dodecylamine (CMC-g-PEG-DDA)

2.2.1. Synthesis of carboxymethyl chitosan-grafted-p(ethylene glycol) (CMC-g-PEG)

PEG-modified chitosans (CMC-g-PEG) were synthesized by a series of coupling reactions between chitosan and monocarboxylated PEG using EDC as coupling agent. First, mPEG–COOH was synthesized with a strong oxidizing agent that converts terminal hydroxyl groups in mPEG to carboxylic acids according to Barrera, Herrera, and Rinaldi (2009), details are described in the supporting information (Fig. S2). Carboxyl groups now available in mPEG–COOH reacted in a second step with $-NH_2$ in CMC via amidation reaction to obtain CMC-g-PEG. In a reaction vessel, mPEG–COOH (1.24 g, 0.62 mmol) and EDC (0.24 g, 1.24 mmol) were dissolved in deionized water (10 mL), and then the CMC (0.1 g, 0.62 mmol glucosamine repeat unit) aqueous solution was added dropwise. The mixture was allowed to react at 25 °C for 24 h. After completion of the reaction, the solution was transferred into a dialysis tube (Mw cut-off of 8000–14,000 Da) and dialyzed against deionized water for two days. The product CMC-g-PEG was dried under a vacuum at 30 °C for 24 h and estimated using ^{1}H NMR (DMSO-d_6). The yield was 50%. The graft level of PEG was calculated with the following equation:

$$\frac{m1 - m2}{m(PEG)}, \quad (1)$$

$m1$, the weight of product; $m2$, the weight of the CMC.

2.2.2. Synthesis of CMC-grafted-p(ethylene glycol)-dodecylamine (CMC-g-PEG-DDA)

As well, the PEG-CMC-DDA was synthesized via the amidation reaction between $-NH_2$ in DDA and –COOH in CMC. Briefly, PEG-g-CMC (0.1 g, 0.09 mmol glucosamine repeat unit) was dissolved in dry DMSO (20 mL), into which EDC (0.02 g, 0.10 mmol) was added. The mixture was stirred at room temperature for 40 min. Next, DDA (3.4 mg, 0.018 mmol, 20% mol substitution with respect to glucosamine repeat unit) was dropped into the mixture wisely. The reaction continued for 24 h at 25 °C. Finally, the solution was transferred into a dialysis tube (Mw cut-off of 8000–14,000 Da) and dialyzed against deionized water for two days. The product CMC-g-PEG-DDA was dried under a vacuum at 30 °C for 24 h and estimated using ^{1}H NMR (DMSO-d_6). The yield was 54.9%.

2.2.3. Characterization techniques

Compound structure was analyzed by ^{1}H nuclear magneticresonance (NMR) spectroscopy with samples dissolved in DMSO-d_6 or D_2O solvent on a Varina Unity-500 (500) MHz spectrometer, using tetramethylsilane as the reference signal. Hydrodynamic diameters (HD) and size distribution of a series of polymeric micelles were determined with dynamic light scattering (DLS) using a Brookhaven BI9000AT system (Brookhaven Instruments Corporation, USA). Molecular weights were recorded on a gel permeation chromatograph (GPC) equipped with two Mixed-B columns (pore size = 10 μm; column size = 300 mm × 7.5 mm) and a refractive index detector (Perkin-Elmer Series 200). The eluent was a 0.1 mol L^{-1} NaCl aqueous solution, and the temperature of the columns was kept at 30 °C. The flow rate was maintained at 0.5 mL min^{-1}, and the sample concentration was 2 mg mL^{-1}.

2.3. Preparation of mineralized polymeric micelles

An amphiphilic polymer (CMC-g-PEG-DDA) can form self-assembled polymeric micelles (PM) due to the hydrophobic interactions between the long alkyl chain of dodecylamine and the hydrophobicity of chitosan backbone. Mineralization of the PM was carried out in the presence of calcium chloride and disodium hydrogen phosphate using a dialysis method and a subsequent mineralization similar to that reported by Min et al. (2012). CMC-g-PEG-DDA (20 mg) was dissolved in 4 mL DMSO. The solution was dialyzed using a membrane bag (Spectrapor, MWCO: 1000) against deionized water. After 24 h, the solution of CMC-g-PEG-DDA (2 mg mL^{-1}) micelles (PM) were collected. To induce calcium phosphate mineralization on polymeric micelles, an aqueous $CaCl_2$ solution (0.5 mL, 2.9 mM) was first added into a stirring solution of PM (1 mL, 2 mg mL^{-1}) and equilibrated for 5 h under stirring at

400 rpm. The molar concentration ratio of [COO^-] to [Ca^{2+}] was 1:0.5 (Perkin et al., 2005). An aqueous solution of Na_2HPO_4 (1 mL, 2.9 mM) was slowly dropped into the reaction mixture, and the solution was stirred magnetically at 400 rpm at room temperature for 12 h. The solution was dialyzed to remove unreacted ionic species and then collected as bare mineralized polymeric micelles (MPM).

DOX-loaded calcium phosphate mineralized micelles were prepared by the dialysis method and subsequent mineralization. Before loading DOX to the CMC-g-PEG-DDA micelles, DOX·HCl (1 mg, 0.0017 mmol) was stirred with TEA (0.31 μL, 0.0022 mmol) in DMSO (1 mL) overnight in the dark. CMC-g-PEG-DDA (10 mg) was dissolved in DMSO (2 mL), and the DOX solution (1 mL) was subsequently added and stirred in the dark at room temperature for 2 h. The solution was dialyzed using a membrane bag (Spectrapor, MWCO: 1000). After 12 h, the solution of DOX-loaded micelles (PM@DOX) was collected. To achieve mineralization of the DOX-loaded polymeric micelles (MPM@DOX), $CaCl_2$ and Na_2HPO_4 were sequentially added into the solution as described above. The UV–vis spectra of MPM@DOX shows the characteristic peak of DOX at 488 nm.

2.3.1. Characterization of mineralized polymeric micelles

Hydrodynamic diameters (HD) and size distribution of different polymeric micelles were determined by dynamic light scattering (DLS) using Brookhaven BI9000AT system (Brookhaven Instruments Corporation, USA). FT-IR spectrum was recorded with a Fourier trans-form infrared spectrometer (Bruker IFS66V FTIR, Germany) in KBr discs. The morphology of polymeric micelles (PM and MPM) and DOX-loaded polymeric micelles (PM@DOX and MPM@DOX) were examined with transmission electron microscopy (TEM) by evaporating one drop of nanocrystal solutions on carbon-coated copper grids. (Hitachi H 8100 transmission electron microscope operating at 200 kV) Energy-dispersive X-ray photoelectron spectroscopy (EDS) measurements were carried out using scanning electron microscopy equipment (SU8020 Hitachi) with a Bruker Energy Dispersive Spectrometer. The contents of the mineral (CaP) were evaluated using Thermo gravimetric analysis (TGA). Samples weighing 3–5 mg were heated from 100 °C to 800 °C at a heating rate of 15 °C min^{-1} in air.

2.3.2. Effect of the pH on the mineralized polymeric micelles

To evaluate the effect of the pH on the MPM, the bare micelles (2 mL, 2 mg mL^{-1}) were incubated in PBS buffer (pH 7.4 or 6.5) or acetate buffer (pH 5.0) (2 mL, 1×). Hydrodynamic diameters were measured by dynamic light scattering at 37 °C at a definite time interval.

2.3.3. Calcium dissolution behavior of mineralized polymeric micelles

The mineralized polymeric micelles solution (4 mL 1 mg mL^{-1}) was sealed in a dialysis membrane bag (MWCO: 3500). The resulting tube was then placed in a release medium (PBS (pH 7.4 or 6.5) or acidic acetate buffer (pH 5.0)(16 mL, 1×), while being shaken at 100 rpm at 37 °C. The release medium (500 μL) was withdrawn at predetermined time intervals and replaced with an equal volume of fresh medium. The release medium (100 μL) was mixed with the Arsenazo III solution (3 mL, 0.15 mmol) in HEPES-buffered saline. The concentration of calcium ions was determined using UV–visible absorption spectroscopy. The absorbance of the solution at 656 nm was then measured, and the concentration of calcium ions was calculated based on the standard curve. To determine the mineralized efficiency, mineralized micelles were stirred in a 1 N HCl solution for 30 min and measured at 656 nm with the Arsenazo III solution, then calculated based on the standard curve.

2.3.4. DOX release from mineralized polymeric micelles

In vitro release profiles of DOX from MPM@DOX were examined in aqueous buffer solutions (pH 7.4, 6.5 of phosphate buffer and pH 5.0 of acetate buffer). MPM@DOX solutions (4 mL, 2 mg mL^{-1}) were transferred into a dialysis membrane bag (MWCO: 3500), and then placed in a release medium (PBS (pH 7.4 or 6.5) or acidic acetate buffer (pH 5.0) (16 mL, 1×). While being stirred at 100 rpm at 37 °C, aliquots (3 mL) of the buffer solutions were taken at certain time intervals and monitored with UV–vis spectrometry at 488 nm to determine the rate of drug release. To determine the drug loading content and loading efficiency, MPM@DOX were stirred in a 1 N HCl solution for 30 min mixed DMSO (vol H_2O:DMSO = 1:4). The DOX concentration was estimated at 488 nm. The drug loading efficiency and loading content were calculated based on the standard curve obtained using free DOX in aqueous solution mixed DMSO (vol. H_2O:DMSO = 1:4) according to the following formulas, respectively.

$$\text{LE\%} = \frac{\text{weight of loading DOX}}{\text{weight of DOX in feed}} \times 100\%$$

$$\text{LD\%} = \frac{\text{weight of loding DOX}}{\text{weight of dry polymer}} \times 100\%$$

3. Results and discussion

3.1. Synthesis and characterization of CMC-g-PEG-DDA

Carboxymethyl chitosan-grafted-p(ethylene glycol)-dodecylamine (CMC-g-PEG-DDA) was synthesized via amidation reaction between $-NH_2$ and $-COOH$ with structure as shown in Fig. 1A. The ^1H NMR (DMSO-d_6) spectra in Fig. S3(A) shows the signals at δ3.521 and those at δ3.252, which are assigned to the methane hydrogen ($-CH_2CH_2O-$) and the methylhydrogen ($-OCH_3$) of the mPEG groups, respectively. This result confirms that products contain mPEG groups. The PEG grafting levels in CMC-g-PEG are 47% calculated by the Eq. (1), which make the products soluble in organic solution and improve the stability of the drug delivery system in the blood. Analogously, in

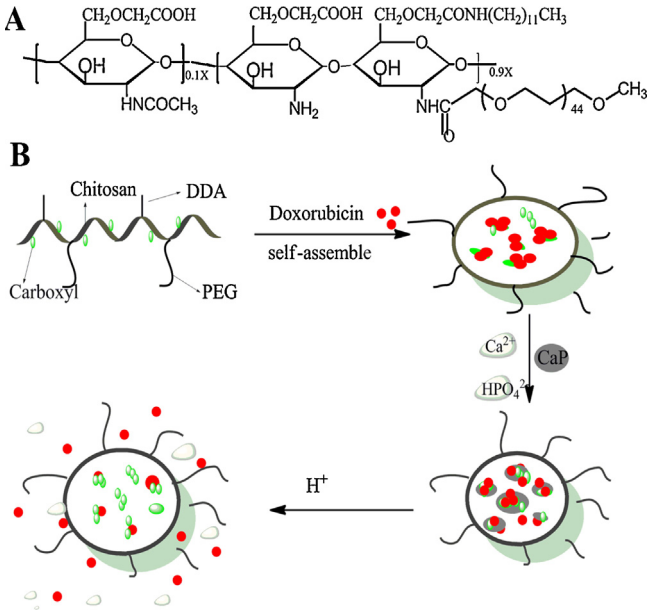

Fig. 1. (A) Structure of amphiphilic chitosan polymer(CMC-g-PEG-DDA). (B) Schematic illustration of the formation of DOX-loaded minerated polymeric micelles.

Table 1
The properties of copolymers.

Sample	Grafting level %	Moleculer weight (Da × 10^4)	Diameter (nm)	Polydisperstiy index
CMC	71	6.1	–	–
CMC-PEG	47	34.6	375.0	0.275
CMC-PEG-DDA	14	35.3	239.7	0.050

comparison with Fig. S3(A), the occurrence of the signals at δ 1.238, 2.115 and at δ 0.854 in the ^{1}H NMR spectrum of the Fig. S3(B) represent the methane hydrogen atoms (–CH_2–) and the methyl hydrogen (–CH_3) of the dodecylamin (DDA) groups, respectively. This suggests that the chitosan derivative carried DDA groups as its side chain successfully, which can control the micelles size and encapsulate a large amount of hydrophobic therapeutic agents. According to the ratio of the peak area at 3.252 ppm to that at 0.854 ppm, the DDA molar substitution degree was estimated 14%. Hydrodynamic sizes (diameters) and the molecular weights of copolymers are shown in Table 1.

3.2. Characterization of mineralized polymeric micelles (MPM)

Unmodified carboxylate groups in the carboxymethyl chitosan backbone have a net surface charge that can make Ca^{2+} deposit on polymeric micelles by electrostatic localization. As a phosphate anion source, Na_2HPO_4 was added into polymeric micelles to induce the growth of nanophase CaP. Fig. 1B illustrates the formation of DOX-loaded mineralized polymeric micelles (MPM@DOX). The FT-IR spectrum of CMC-g-PEG-DDA and its mineralized conjugates were also measured. As shown in Fig. 2A, the bands at 1030 cm^{-1} and 607 cm^{-1} could be attributed to P–O asymmetric stretching and O–P–O bending modes, respectively, which support the presence of CaP on the mineralized conjugates.

Fig. 2B shows the EDS spectra of CaP-mineralized nanoparticles for analysis of major compounds. Signals for Ca and P appear in the EDS spectra, implying that CaP formed on the nanoparticles. The inset shows the selected-area electron diffraction pattern of MPM. No sharp electron diffraction rings were observed, suggesting the formation of amorphous CaP. This is often observed in the early stage of template-induced mineralization.

In addition, the hydrodynamic size distributions of the micelles were investigated by dynamic light scattering (DLS), as shown in Fig. 2C. All polymeric micelles are monodisperse. The average hydrodynamic sizes are 239.7, 138.7, 260 and 161.7 nm for PM, MPM, PM@DOX, and MPM@DOX respectively. Interestingly, the mean diameters of the MPM and MPM@DOX were significantly lower than that of the PM and PM@DOX. This indicates that mineralization of the PM decreased the micelles' size. This might be due to the electrostatic interactions between calcium ions and carboxylates at the backbone of CMC, resulting in the formation of compact nanoparticles micelles. For both the PM and MPM, encapsulation of DOX slightly increased the particle sizes. The obvious change of the hydrodynamic size distributions also indicates the success of mineralization.

Thermogravimetric analysis (TGA) curves further confirm the formation of CaP. As shown in Fig. 2D, TGA curves indicate that the mass-loss profile of the CMC-g-PEG-DDA differs from that of the CaP-mineralized CMC-g-PEG-DDA. In particular, at high temperatures above 600 °C, the mineralized CMC-g-PEG-DDA produces a larger amount of residue than the CMC-g-PEG-DDA, due to the presence of inorganic CaP. The amount of inorganic content in the CaP-mineralized conjugates was estimated as shown in Table 2.

Fig. 3 shows the TEM images of polymeric micelles (PM) and mineralized polymeric micelles (MPM). As expected, all of the micelles were spherical in shape. Interestingly, the multi-core was

Table 2
The characteristics of polymer micelles.

Sample	D^a/nm	ME[b]%	MC[c]%	LE[c]%	LC[d]%
PM	239.7	–	–	–	–
MPM	138.7	71.7	3.2	–	–
PM@DOX	260	–	–	78	6.5
MPM@DOX	161.7	69	2.9	71.2	6.0

[a] Diameter measured using DLS.
[b] Mineralized efficiency determined using UV–visible spectroscopy.
[c] Loading efficiency.
[d] Loading content determined using UV–visible spectroscopy.
[e] Mineral content estimated using TGA.

clearly observed inside the MPM. After mineralization, the sizes of micelles reduced significantly, which is consistent with DLS results, as shown in Fig. 2C. Results also show that the size of nanoparticles measured with DLS is larger than that observed in TEM images. This result is reasonable, since the hydrodynamic size is obtained while particles are dispersed in solution, and aggregation may occur. However, TEM provides the size of the particles after complete drying. Significant changes in morphology and hydrodynamic size also confirm that CaP is brought into polymeric micelles.

Fig. S4 shows the UV–vis spectrum using the characteristic peak of 488 nm of the DOX. A characteristic peak also can be seen after mineralization, implying that mineralization had no influence on the property of DOX.

3.3. Stability analysis dependent on pH

The polymeric micelles' sizes were monitored at 37 °C as a function of time in buffer solutions of different pH values. (Fig. 4) A PBS solution (pH 7.4) was employed to imitate the physiologic pH in normal extracellular environments, whereas a PBS buffer (pH 6.5) and an acetate buffer (pH 5.0) were used to observe the effect of mildly acidic environments, such as intracellular compartments (e.g., endosome and lysosome) and the extracellular matrix of tumor tissue. As shown in Fig. 4, regardless of the pH value, the bare polymeric micelles without mineralization did not change size significantly for up to 7 days. This indicates that pH did not affect the size of the bare polymeric micelles. On the other hand, the size of the MPM is dependent upon pH. At pH 7.4, MPM did not change significantly in size for the entire test time, confirming that mineralized polymeric micelles are stable under the physiologic pH. However, when the MPM was exposed to pH = 5.0 for only one day, the mean sizes increased appreciably, similar to that of bare polymeric micelles. At pH 6.5, the mineralized polymeric micelles' size also increased after one day, whereas the average size for the remaining time period is slightly smaller than that of MPM exposed to pH 5.0. Results are closely related to the dissolution behavior of calcium ions.

3.4. Calcium dissolution behavior of mineralized polymeric micelles

To support the release profiles of DOX from MPM@DOX, a calcium dissolution assay using the Arsenazo III method was performed at different pH conditions. The release patterns of calcium ion from MPM are shown in Fig. 5A. The MPM underwent minimal dissolution (<5%) under the physiological pH condition after 12 h, which can be expected from the premature amorphous CaP of high water solubility. In contrast, under the low pH condition (pH = 5.0), accelerated dissolution of CaP was found after 1 h (>70%). The release rate of calcium ions from the MPM decreased with the increasing of the buffer pH. This pattern of calcium ion release strongly supports the size change (Fig. 4) and the drug release behavior of the particles (Fig. 6). Fig. 5B shows the absorption

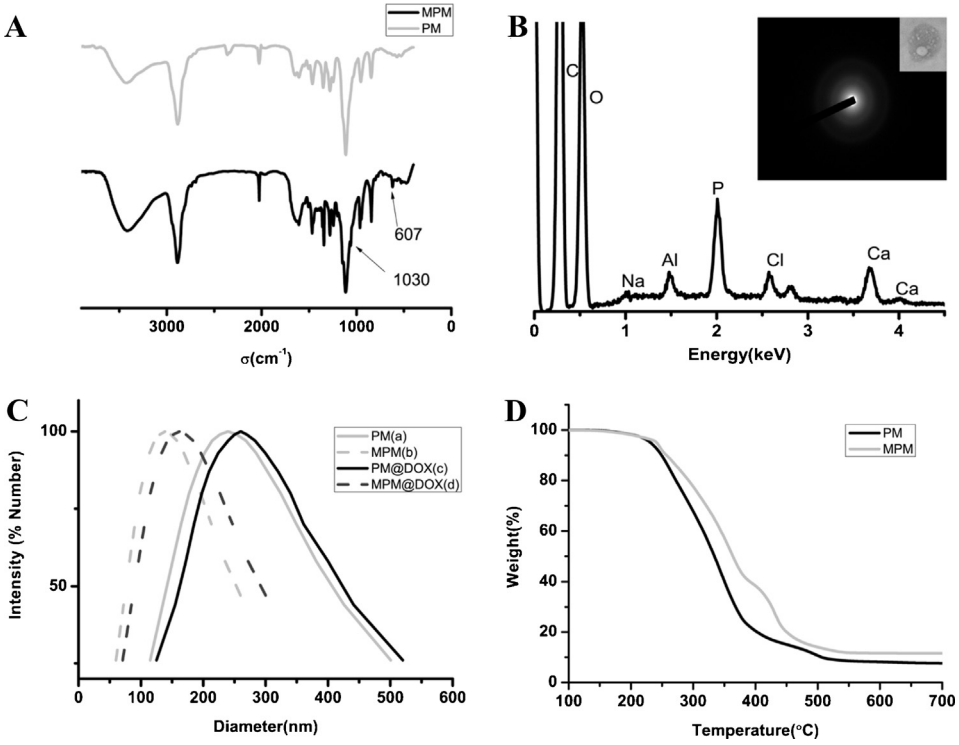

Fig. 2. (A) FT-IR spectrum of CMC-g-PEG-DDA conjugates and its mineralized nanoparticles. (B) SEM-EDS of mineralized nanoparticles, Incet is selected-area electron diffraction pattern of MPM. (C) Size distributions of a serious of micelles estimated by dynamic light scattering. (D) TGA curves of the CMC-g-PEG-DDA conjugates and its mineralize nanoparticles.

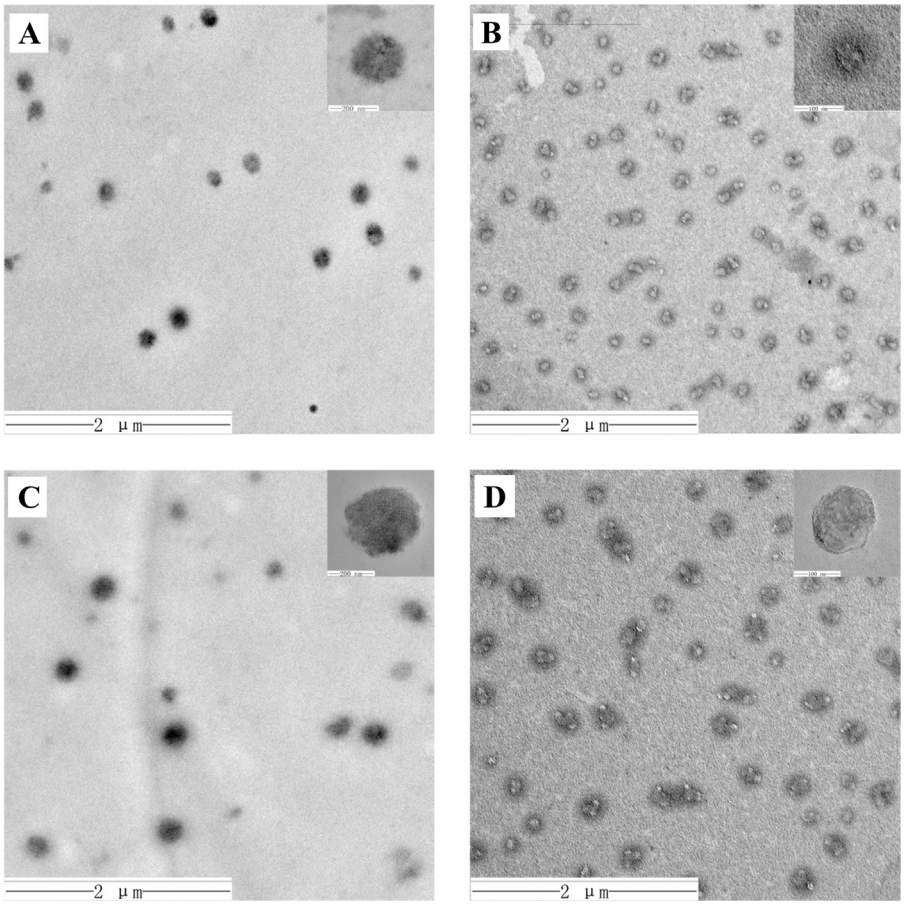

Fig. 3. TEM images of (A) polymer miceller(PM), (B) mineralized polymer micelles(MPM), (C) DOX-loaded polymer micelles(PM@DOX), (D) DOX-loaded mineralized polymer micelles(MPM@DOX). Insets are magnified images.

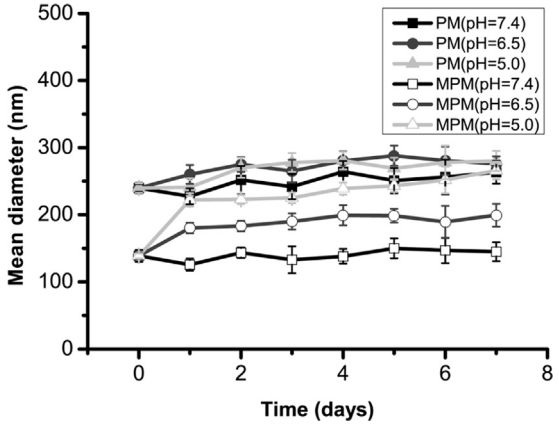

Fig. 4. Polymer micelles' size in buffer solutions at 37 °C as a function of time. The error bars in the graph represent standard deviations ($n = 3$).

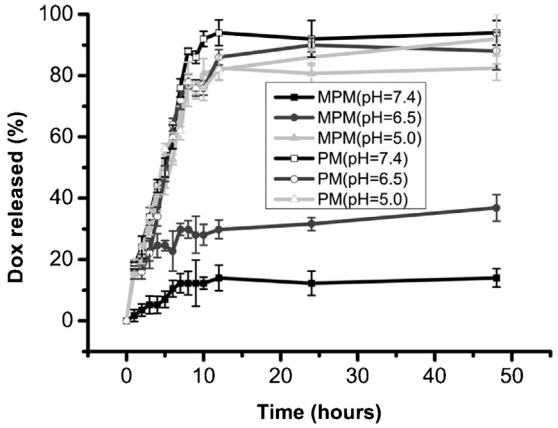

Fig. 6. DOX release profiles from PM@DOX and MPM@DOX under pH control. The error bars in the graph represent standard deviations ($n = 3$).

spectrum of Arsenazo III/Ca^{2+} complex of MPM at different pH values after incubating for 4 h. The release behavior of the calcium ion from MPM is highly evident.

3.5. Drug release behavior

For the pH-controlled DOX release from MPM@DOX, we employed pH variation in the aqueous buffer solutions (pH 7.4 and 6.5 phosphate buffer and pH 5.0 acetate buffer). Fig. 6. shows the release kinetics of DOX from PM@DOX and MPM@DOX, respectively. In general, DOX was rapidly released from the nanoparticles in initial 8 h, followed by a slower release for the remaining period of time. The bare PM@DOX released over 85% of the DOX in 2 days under any pH of the buffer solution, regardless of the pH value. On the other hand, MPM@DOX shows a pH-dependent DOX release pattern. Drug release was effectively inhibited in mineralized micelles at pH 7.4 (<20%), whereas shows a general release trend at pH 5.0 (>80%). In addition, the release rate of DOX from the MPM@DOX decreased as the buffer pH increased. These results are closely related to the behavior of calcium dissolution, as shown in Fig. 5. Loading efficiency and loading content are shown in Table 2. Collectively, results show that MPM@DOX can not only minimize drug loss in the blood, but also release the drugs for therapeutic effects once they are internalized within the target cells. In terms of the delivery efficiency, the MPM@DOX shows more promise than the native non-mineralized PM@DOX.

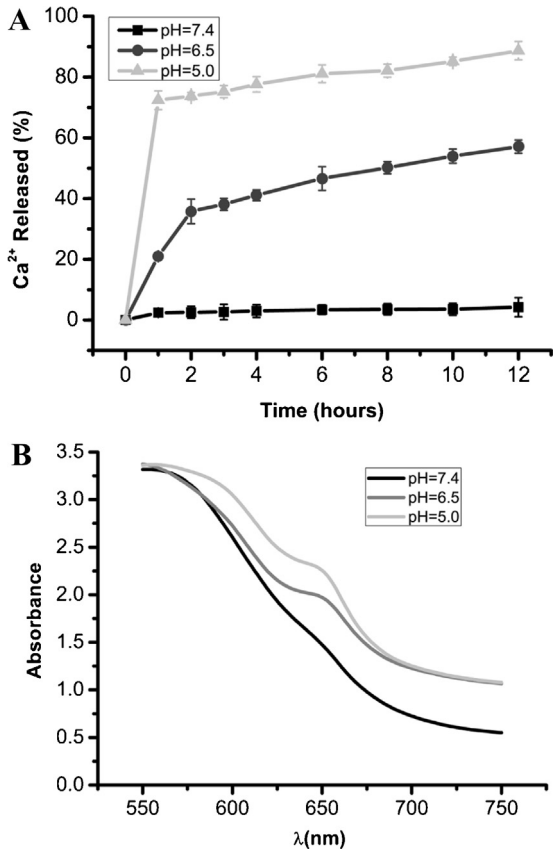

Fig. 5. (A) Kinetics of calcium dissolution from MPM under pH control. (B) Absorption spectra of Arsenazo III/Ca^{2+} complex after 4 h of incubation of MPM at different pH values. The error bars in the graph represent standard deviations ($n = 3$).

4. Conclusion

Our group successfully synthesized an amphiphilic chitosan derivative (CMC-g-PEG-DDA) and prepared a robust pH-sensitive drug carrier by controlled deposition of calcium and phosphate ions. This mineralized polymeric micelles shows a narrower particle-size distribution and higher colloidal stability in solution compared to bare polymeric micelles. Moreover, this system exhibited several attractive features, including high drug-loading capacity, mild storage-release conditions, and pH-sensitive drug-release behavior. Therefore, this can be considered as an exciting alternative to the polymeric delivery system in the cancer therapy.

Acknowledgements

This work is supported financially by the Natural Science Foundation of China (No. 20904014), the Science Foundation for Youths of Jilin Committee of Science and Technology (No. 20080119), the Fund for Doctoral Program of Chinese Ministry of Education (No. 20090061110017) and the Fund for Youths of Chinese Ministry of Education (No. 2070310).

Appendix A. Supplementary data

Supplementary data associated with this article can be found, in the online version, at http://dx.doi.org/10.1016/j.carbpol.2014.04.082.

References

Adams, M. L., Lavasanifar, A., & Kwon, G. S. (2003). Amphiphilic block copolymers for drug delivery. *Journal of Pharmaceutical Sciences, 92*, 1343–1355.

Angelos, S., Yang, Y. W., Patel, K., Stoddart, J. F., & Zink, J. I. (2008). pH-responsive supramolecular nanovalves based on cucurbituril pseudorotaxanes. *Angewandte Chemie International Edition*, *120*, 2254–2258.

Bae, Y. H., & Yin, H. Q. (2008). Stability issues of polymeric micelles. *Journal of Controlled Release*, *131*, 2–4.

Barrera, C., Herrera, A. P., & Rinaldi, C. (2009). Colloidal dispersions of monodisperse magnetite nanoparticles modified with poly(ethylene glycol). *Journal of Colloids and Interface Science*, *329*, 107–113.

Choi, K. Y., Chung, H., Min, K. H., Yoon, H. Y., Kim, K., Park, J. H., et al. (2010). Self-assembled hyaluronic acid nanoparticles for active tumor targeting. *Biomaterials*, *31*, 106–114.

Epple, M., Ganesan, K., Heumann, R., Klesing, J., Kovtun, A., Neumann, S., et al. (2010). Application of calcium phosphate nanoparticles in biomedicine. *Journal of Materials Chemistry*, *20*, 18–23.

Fan, L., Li, F., Zhang, H., Wang, Y., Cheng, C., Li, X., et al. (2010). Co-delivery of PDTC and doxorubicin by multifunctional micellar nanoparticles to achieve active targeted drug delivery and overcome multidrug resistance. *Biomaterials*, *31*, 5634–5642.

Han, H. S., Lee, J., Kim, H. R., Chae, S. Y., Kim, M., Saravanakumar, G., et al. (2013). Robust PEGylated hyaluronic acid nanoparticles as the carrier of doxorubicin: Mineralization and its effect on tumor targetability in vivo. *Journal of Controlled Release*, *168*, 105–114.

Hiki, S., & Kataoka, K. (2007). A facile synthesis of azido-terminated heterobifunctional poly(ethyleneglycol)s for click conjugation. *Bioconjugate Chemistry*, *18*, 2191–2196.

Hu, F. Q., Meng, P., Dai, Y. Q., Du, Y. Z., You, J., Wei, X. H., et al. (2008). PEGylated chitosan-based polymer micelle as an intracellular delivery carrier for anti-tumor targeting therapy. *European Journal of Pharmaceutics and Biopharmaceutics*, *70*, 749–757.

Kurita, K. (2001). Controlled functionalization of the polysaccharide chitin. *Progress in Polymer Science*, *26*, 1921–1971.

Lee, H. J., Kim, S. E., Kwon, K., Park, C., Kim, C., Yangc, J., et al. (2010). Spatially mineralized self-assembled polymeric nanocarriers with enhanced robustness and controlled drug-releasing property. *Chemical Communications*, *46*, 377–379.

Li, W. M., Chen, S. Y., & Liu, D. M. (2013). In situ doxorubicin–CaP shell formation on amphiphilic gelatin–iron oxide core as a multifunctional drug delivery system with improved cytocompatibility, pH-responsive drug release and MR imaging. *Acta Biomaterialia*, *9*, 5360–5368.

Min, K. H., Lee, H. J., Kim, K., Kwon, I. C., Jeong, S. Y., & Lee, S. C. (2012). The tumor accumulation and therapeutic efficacy of doxorubicin carried in calcium phosphate-reinforced polymer nanoparticles. *Biomaterials*, *33*, 5788–5797.

Onaca, O., Enea, R., Hughes, D. W., & Meier, W. (2009). Stimuli-responsive polymersomes as nanocarriers for drug and gene delivery. *Macromolecular Bioscience*, *9*, 129–139.

Perkin, K. K., Turner, J. L., Wooley, K. L., Mann, S., & Stephen, M. (2005). Fabrication of hybrid nanocapsules by calcium phosphate mineralization of shell cross-linked polymer micelles and nanocages. *Nano Letters*, *5*(7), 1457–1461.

Qutachi, O., Shakesheff, K. M., & Buttery, L. D. K. (2013). Delivery of definable number of drug or growth factor loaded poly(DL-lactic acid-co-glycolic acid) microparticles within human embryonic stem cell derived aggregates. *Journal of Controlled Release*, *168*, 18–27.

Rim, H. P., Min, K. H., Lee, H. J., Jeong, S. Y., & Lee, S. C. (2011). pH-tunable calcium phosphate covered mesoporous silica nanocontainers for intracellular controlled release of guest drugs. *Angewandte Chemie International Edition*, *50*, 8853–8857.

Schmidt, H. T., & Ostafin, A. E. (2002). Liposome directed growth of calcium phosphate. *Advanced Materials*, *14*(7), 532–535.

Shi, B. Y., Shen, Y. Z., Zhang, H., Bi, J. X., & Dai, S. (2012). Exploring N-imidazolyl-O-carboxymethyl chitosan for high performance gene delivery. *Biomacromolecules*, *13*, 146–153.

Shi, J., Votruba, A. R., Farokhzad, O. C., & Langer, R. (2010). Nanotechnology in drug delivery and tissue engineering: from discovery to applications. *Nano Letters*, *10*, 3223–3230.

Sugawara, A., Yamane, S., & Akiyoshi, K. (2006). Nanogel-templated mineralization: Polymer-calcium phosphate hybrid nanomaterials. *Macromolecular Rapid Communications*, *27*, 441–446.

Wang, Z., Zhou, C., Xia, J., Via, B., Xia, Y., Zhang, F., et al. (2013). Fabrication and characterization of a triple functionalization of graphene oxide with Fe_3O_4, folic acid and doxorubicin as dual-targeted drug nanocarrier. *Colloids and Surfaces B: Biointerfaces*, *106*, 60–65.

Yao, Z., Zhang, C., Ping, Q., & Yu, L. (2007). A series of novel chitosan derivatives: Synthesis, characterization and micelle solubilization of paclitaxel. *Carbohydrate Polymers*, *68*, 781–792.

Yuk, S. H., Oh, K. S., Cho, S. H., Kim, S. Y., Oh, S., Lee, J. H., et al. (2012). Enhancement of the targeting capabilities of the paclitaxel-loaded pluronic nanoparticles with a glycol chitosan/heparin composite. *Molecular Pharmaceutics*, *9*, 230–236.